Research Article | Vol. 8, No. 3 | 1 Mar 2018 | OPTICAL MATERIALS EXPRESS 698

Optical Materials EXPRESS

Enhanced nonlinear optical properties of reduced graphene oxide decorated with silver nanoparticles

MENGMENG YUE, JINHAI SI,* LIHE YAN, YANG YU, AND XUN HOU

Key Laboratory for Physical Electronics and Devices of the Ministry of Education & Shaanxi Key Lab of Information Photonic Technique, School of Electronics & Information Engineering, Xi'an Jiaotong University, Xi'an, 710049, China

**jinhaisi@mail.xjtu.edu.cn*

Abstract: Reduced graphene oxide (rGO) decorated with silver nanoparticles (Ag NPs) is synthesized by femtosecond laser ablation in solution method. The nonlinear optical properties of both rGO and Ag NPs/rGO are measured using a femtosecond laser Z-scan technique. The results reveal that both the nonlinear absorption and nonlinear refraction in the hybrid are enhanced due to the interaction of the energy state of Ag NPs. The composite shows a saturation intensity 18.5 MW/cm2 and boosts the nonlinear refraction as large as 2~3 times of that of rGO reaching to -1.1×10^{-12} m^2/W. The enhancement of the saturable absorption might be caused by the further bleaching the valence band of rGO due to the transfer of the light excited carriers from graphene to the metal state of the NPs. The slow relaxation of the excited carriers to the ground state of rGO will also cause the increase of the carrier density and thereby result in the enhancement of the nonlinear refractive index of the material.

OCIS codes: (190.4400) Nonlinear optics, materials; (310.6860) Thin films, optical properties; (320.7110) Ultrafast nonlinear optics.

References and links

1. A. Dahal and M. Batzill, "Graphene-nickel interfaces: a review," Nanoscale **6**(5), 2548–2562 (2014).
2. D. Zhang, M. Lau, S. Lu, S. Barcikowski, and B. Gökce, "Germanium Sub-Microspheres Synthesized by Picosecond Pulsed Laser Melting in Liquids: Educt Size Effects," Sci. Rep. **7**, 40355 (2017).
3. A. C. Neto, F. Guinea, N. M. Peres, K. S. Novoselov, and A. K. Geim, "The electronic properties of graphene," Rev. Mod. Phys. **81**(1), 109–162 (2009).
4. N. Liaros, A. B. Bourlinos, R. Zboril, and S. Couris, "Fluoro-graphene: nonlinear optical properties," Opt. Express **21**(18), 21027–21038 (2013).
5. H. Chang, Z. Sun, Q. Yuan, F. Ding, X. Tao, F. Yan, and Z. Zheng, "Thin Film Field-Effect Phototransistors from Bandgap-Tunable, Solution-Processed, Few-Layer Reduced Graphene Oxide Films," Adv. Mater. **22**(43), 4872–4876 (2010).
6. J. Zhu, Y. Li, Y. Chen, J. Wang, B. Zhang, J. Zhang, and W. J. Blau, "Graphene oxide covalently functionalized with zinc phthalocyanine for broadband optical limiting," Carbon **49**(6), 1900–1905 (2011).
7. M. K. Kavitha, H. John, P. Gopinath, and R. Philip, "Synthesis of reduced graphene oxide–ZnO hybrid with enhanced optical limiting properties," J. Mater. Chem. C Mater. Opt. Electron. Devices **1**(23), 3669–3676 (2013).
8. T. V. Thu, P. J. Ko, N. H. Phuc, and A. Sandhu, "Room-temperature synthesis and enhanced catalytic performance of silver-reduced graphene oxide nanohybrids," J. Nanopart. Res. **15**(10), 1975 (2013).
9. B. S. Kalanoor, P. B. Bisht, S. A. Ali, T. T. Baby, and S. Ramaprabhu, "Optical nonlinearity of silver-decorated graphene," J. Opt. Soc. Am. B **29**(4), 669–675 (2012).
10. B. Anand, A. Kaniyoor, S. S. S. Sai, R. Philip, and S. Ramaprabhu, "Enhanced optical limiting in functionalized hydrogen exfoliated graphene and its metal hybrids," J. Meter. Chem. C **1**(15), 2773–2780 (2013).
11. C. Li, X. Shi, J. Si, T. Chen, F. Chen, A. Li, and X. Hou, "Fabrication of three-dimensional microfluidic channels in glass by femtosecond pulses," Opt. Commun. **282**(4), 657–660 (2009).
12. L. Yan, J. Yue, J. Si, and X. Hou, "Influence of self-diffraction effect on femtosecond pump-probe optical Kerr measurements," Opt. Express **16**(16), 12069–12074 (2008).
13. V. Nguyen, L. Yan, H. Xu, and M. Yue, "One-step synthesis of multi-emission carbon nanodots for ratiometric temperature sensing," Appl. Surf. Sci. **427**, 1118–1123 (2018).
14. D. Tan, X. Liu, Y. Dai, G. Ma, M. Meunier, and J. Qiu, "A Universal Photochemical Approach to Ultra-Small, Well-Dispersed Nanoparticle/Reduced Graphene Oxide Hybrids with Enhanced Nonlinear Optical Properties," Adv. Opt. Mater. **3**(6), 836–841 (2015).

#319010 https://doi.org/10.1364/OME/8.000698
Journal © 2018 Received 3 Jan 2018; revised 14 Feb 2018; accepted 14 Feb 2018; published 28 Feb 2018

Optical Materials EXPRESS

15. D. Werner and S. Hashimoto, "Controlling the pulsed-laser-induced size reduction of Au and Ag nanoparticles via changes in the external pressure, laser intensity, and excitation wavelength," Langmuir **29**(4), 1295–1302 (2013).
16. M. Sheik-Bahae, A. A. Said, T. H. Wei, D. J. Hagan, and E. W. Van Stryland, "Sensitive measurement of optical nonlinearities using a single beam," IEEE J. Quantum Electron. **26**(4), 760–769 (1990).
17. J. I. Paredes, S. Villar-Rodil, A. Martínez-Alonso, and J. M. D. Tascón, "Graphene oxide dispersions in organic solvents," Langmuir **24**(19), 10560–10564 (2008).
18. Z. Sun, N. Dong, K. Wang, D. König, T. C. Nagaiah, M. D. Sánchez, and M. Muhler, "Ag-stabilized few-layer graphene dispersions in low boiling point solvents for versatile nonlinear optical applications," Carbon **62**, 182–192 (2013).
19. S. Stankovich, R. D. Piner, X. Chen, N. Wu, S. T. Nguyen, and R. S. Ruoff, "Stable aqueous dispersions of graphitic nanoplatelets via the reduction of exfoliated graphite oxide in the presence of poly (sodium 4-styrenesulfonate)," J. Mater. Chem. **16**(2), 155–158 (2006).
20. H. Shi, C. Wang, Z. Sun, Y. Zhou, K. Jin, S. A. Redfern, and G. Yang, "Tuning the nonlinear optical absorption of reduced graphene oxide by chemical reduction," Opt. Express **22**(16), 19375–19385 (2014).
21. G. Williams, B. Seger, and P. V. Kamat, "TiO_2-graphene nanocomposites. UV-assisted photocatalytic reduction of graphene oxide," ACS Nano **2**(7), 1487–1491 (2008).
22. P. Aloukos, I. Papagiannouli, A. B. Bourlinos, R. Zboril, and S. Couris, "Third-order nonlinear optical response and optical limiting of colloidal carbon dots," Opt. Express **22**(10), 12013–12027 (2014).
23. X. F. Jiang, L. Polavarapu, S. T. Neo, T. Venkatesan, and Q. H. Xu, "Graphene oxides as tunable broadband nonlinear optical materials for femtosecond laser pulses," J. Phys. Chem. Lett. **3**(6), 785–790 (2012).
24. K. S. Subrahmanyam, A. K. Manna, S. K. Pati, and C. N. R. Rao, "A study of graphene decorated with metal nanoparticles," Chem. Phys. Lett. **497**(1), 70–75 (2010).
25. S. Kumar, M. Anija, N. Kamaraju, K. S. Vasu, K. S. Subrahmanyam, A. K. Sood, and C. N. R. Rao, "Femtosecond carrier dynamics and saturable absorption in graphene suspensions," Appl. Phys. Lett. **95**(19), 191911 (2009).
26. Y. Fan, Z. Jiang, and L. Yao, "Two-photon absorption of monolayer graphene suspensions in femtosecond regime," Chin. Opt. Lett. **10**(7), 071901 (2012).
27. M. Saravanan, T. S. Girisun, G. Vinitha, and S. V. Rao, "Improved third-order optical nonlinearity and optical limiting behaviour of (nanospindle and nanosphere) zinc ferrite decorated reduced graphene oxide under continuous and ultrafast laser excitation," RSC. Adv. **6**(94), 91083–91092 (2016).

1. Introduction

Materials with large third-order optical nonlinearity and ultrafast nonlinear optical (NLO) response are of great importance for photonic applications such as optical shutter, optical limiting, information processing, and so on [1–3]. As a star material, graphene has raised more and more significant concern for its excellent optical properties. As the interband optical transitions in graphene are independent of incident light wavelength over a wide range, it has exhibited unique NLO properties such as nonlinear absorption and nonlinear refraction effects [4]. The abundant oxygen-containing groups in graphene oxide (GO) enables its easy functionalization with various functional materials such as organic molecules and inorganic nanomaterials [5–8]. The synergistic effects of GO and the functionalizing materials improve their NLO performances significantly. Although some researchers have demonstrated the enhanced NLO properties of functionalized GO materials using nanosecond and picosecond pulses [9, 10], the NLO response of reduced graphene oxide (rGO) decorated with noble metal NPs in femtosecond regime is still unclear and need further investigations.

Femtosecond laser ablation in solution (FLAS) method can provide a green synthesis strategy of metal/graphene nanocomposites. Due to its ultra-short pulse duration and ultra-high peak power, femtosecond laser pulses have been used in micro-fabrication and ultrafast measurements areas [11–13]. When femtosecond laser irradiates GO aqueous solution containing metal ions, plasma plumes are produced and reactions between these species result in NPs formation, as well as the reduction and doping of GO [14, 15]. The FLAS synthetized metal NPs with nanometer sizes are naturally and uniformly doped on the rGO sheets without any further treatment. Compared with the conventional chemical functionalization methods, FLAS is more time-saving, easily operated, and avoids the usage of harmful chemical reagents.

In this paper, silver NPs and rGO (Ag NPs/rGO) nanocomposites are synthesized using FLAS method. The as prepared Ag NPs/rGO hybrids are characterized by absorption spectra, TEM images, and XPS spectra. Femtosecond laser Z-scan measurements are performed to study the ultrafast NLO response of the materials. The results reveal both nonlinear

Optical Materials EXPRESS

absorption and nonlinear refraction can be effectively enhanced by the hybridization of Ag NPs. The Ag NPs/rGO shows lower saturation intensity (18.5 MW/cm^2) and boosts the nonlinear refraction as large as 2~3 times of that of rGO reaching to -1.1×10^{-12} m^2/W, which are attributed to the interaction of the state of metal. When rGO decorated with AgNPs and excited by the laser pulse, excited carriers probably transfer to the metal and then relax to the ground state of rGO. The relative slow relaxation of the excited carriers from the metal states to the VB of rGO will cause the increase of the carrier density in the excited states, resulting in enhancements of the saturable absorption and nonlinear refraction.

2. Experimental setup

GO used in our experiments was obtained from Nanjing XFNano Materials Tech Co., Ltd., (Nanjing, China). The synthetic procedures of Ag NPs/rGO were as following: First, 2 mg GO was dispersed in 10 ml of distilled water by ultrasonicate for 1 hour until a uniform yellow 0.2 mg/ml rGO solution was obtained. Next, 0.01 mmol $AgNO_3$ was added into the solution and ultrasonicated again. During the reduction process, a Ti: sapphire amplifier system emitting 80 fs laser pulses centered at 800 nm at a repetition of 1 kHz was used. The laser beam was focused into the mixture suspension by a 100 mm lens for 30 min. The laser power was fixed at 100 mW. During the laser reduction process, a magnetic stirrer was used to make the solution to be irradiated homogenously. The samples (GO, rGO and Ag NPs/rGO) were deposited on 1 mm thick glass substrate and dried at room temperature.

Morphological properties of the produced Ag NPs/rGO material were studied by transmission electron microscopy (TEM) and high resolution TEM (HRTEM) using a JEM-ARM200F microscope. Elemental composition analysis was carried out by X-ray photoelectron spectroscopy (XPS) using an AXIS ULtrabld XPS spectrometer. UV-Vis absorption spectra were obtained using a UV-2600 spectrophotometer.

Femtosecond Z-scan measurements were employed to study the NLO response of the produced materials. Femtosecond pulses emitted from the same amplifier system mentioned above were used as the laser source in the experiments. The Z-scan setup was similar as descripted in some previous reports [16]. Laser pulses were focused using an f = 300 mm lens and the sample was mounted on a translation stage that moved along the z-axis with respect to the focus of the lens. As the sample was moved closer to focus for a distance far away, the laser irradiance increased, leading to self-focusing (or self-defocusing) in the sample. As a result, the laser power transmitting through the adjustable aperture in front of the power meter varied as a function of the Z-position. This arrangement allowed us to perform the open-aperture (OA) Z-scan and closed aperture (CA) Z-scan measurements, which was used to determine the nonlinear absorption and nonlinear refraction effect in the sample, respectively.

3. Results and discussion

Firstly, the characterizations of the as-prepared Ag NPs/rGO composites were carried out by UV-Vis spectroscopy, TEM and XPS analysis. Figure 1(a) shows the UV-Vis absorption spectra of the rGO, Ag NPs/rGO and the reference sample of GO. The characteristic shoulder of GO absorption spectra at 305 nm is attributed to the $n \rightarrow \pi^*$ transitions of C = O bonds [17]. After laser irradiation, the absorption shoulder at 305 nm of rGO disappears and the absorption in the whole visible light range increases, indicating the reduction of GO. The absorption spectra of Ag NPs/rGO shows the similar profile as that of the rGO and a strong absorption band at around 410 nm, which can be attributed to the localized surface plasmon resonance of Ag NPs [18].

Figure 1 (b) shows the typical TEM image of Ag NPs/rGO hybrid. The as-prepared Ag NPs (as shown by the black dots) are well dispersed on the rGO nanosheets. Figure 1 (c) indicates the size distribution of Ag NPs, which is in a range of 3-22 nm. As shown in Fig. 1 (d), the HRTEM image of Ag NPs exhibits obvious crystal lattice fringe with the spacing of 0.23 nm, which is nearly the same as that of (111) plane of the Ag crystallite.

Optical Materials EXPRESS

XPS spectra of GO and Ag NPs/rGO are depicted in Fig. 2(a) and (b) respectively. The C-C binding energy is assigned at 284.8 eV. Chemical shifts of + 1.4, + 3.0 eV are assigned for C-O and C = O groups [19]. In both samples, XPS spectra are well fitted with sub-peaks corresponding to functional groups. The percentage area of each sub-peak for GO and Ag NPs/rGO are obtained. The percentage of C = C, C-O and C = O for the GO are calculated to be 48.49%, 40.24% and 11.26%, while those for the Ag NPs/rGO are 62.94%, 26.25%and 7.08%. These results suggest significant removal of oxygen functional groups after laser reduction process. Compared with the XPS results of rGO prepared using some other methods [19–21], the products prepared using laser ablation method show a comparable reduction degree.

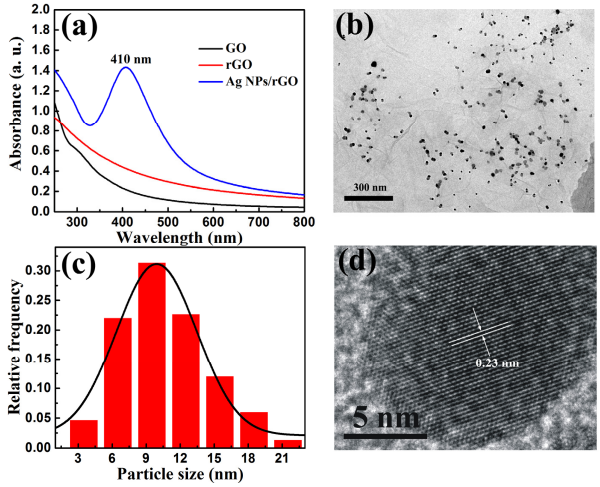

Fig. 1. (a) UV-Vis absorption spectra of the GO, rGO and Ag NPs/rGO. (b) TEM images of Ag NPs/rGO. (c) The size distribution of Ag NPs. and (b) HRTEM images of Ag NPs.

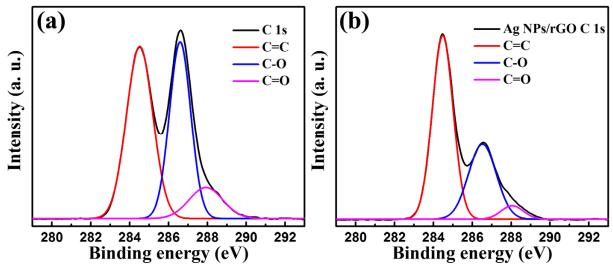

Fig. 2. XPS spectra of (a) GO and (b) Ag NPs/rGO.

Nonlinear absorption of rGO and Ag NPs/rGO were characterized using an OA Z-scan measurement. The radius of laser spot was estimated to be about 25 μm and the highest corresponding peak intensity was about 45 MW/cm^2. The black squares and red circles in Fig. 3(a) show the OA Z-scan measurement results of rGO and Ag NPs/rGO, respectively. According to the nonlinear optical theory, the OA Z-scan curves in both samples are fitted using the formula [22]:

$$T = \frac{1}{\sqrt{\pi}\,\beta I_0 L_{eff} / (1 + z^2 / z_{\mathrm{R}}^2)} \int_{-\infty}^{+\infty} \ln[1 + \frac{\beta I_0 L_{eff}}{(1 + z^2 / z_R^2)} \exp(-t^2)] dt \qquad (1)$$

where, T, I_0 and Z_R stand for the normalized transmittance, the peak light intensity at the focus and the Rayleigh length of the beam, respectively. L_{eff} and β represent the effective length of the sample and the nonlinear absorption coefficient of the sample. From the figure

Optical Materials EXPRESS

we can see that, both the normalized transmittances are increased as the samples move forwards to the beam focus (z = 0), exhibiting an obvious SA behavior. Besides, the Ag NPs/rGO exhibits an enhanced SA behavior compared to that of rGO. To confirm the enhancement of optical nonlinearities of rGO functionalized with Ag NPs, we measured the nonlinear transmission measurement of rGO and Ag NPs/rGO as functions of the light intensity. The results are plotted in Fig. 3(b) and fitted theoretically using the following equations:

$$T_L = 1 - \alpha_0 \tag{2}$$

$$T_{NL} = 1 - \alpha_0 / (1 + I/I_s) \tag{3}$$

Where T_L is the linear transmittance, T_{NL} is the nonlinear transmittance, I is the light peak intensity, I_S is the saturation intensity and α_0 is the linear absorption coefficient. In the fitting process the linear optical losses caused by reflection and scattering of the sample are considered. Based on the fitted results, the saturation intensity I_S of rGO and Ag NPs/rGO can be obtained, which are evaluated to be 25.1 MW/cm^2 and 18.5 MW/cm^2, respectively.

Here, we give a brief interpretation for the enhanced SA effect in Ag NPs/rGO composites. Firstly, the effect of local field enhancements could be ruled out. By comparing the SA effects for two samples given in Fig. 3(b) we can find that, the modulation depth of rGO is still much lower than that of Ag NPs/rGO even when the incident laser intensity is much higher. This indicates that the enhancement of the laser field cannot cause such a huge increase of the SA effect in the hybrid. The improvement of the SA of the hybrid could be attributed to the charge transfer between Ag NPs and rGO. Because rGO has a zero bandgap, large transient populations of carriers in the conduction band (CB) and valence band (VB) are created when the laser irradiates on the material. As the pulse duration is comparable with the interband relaxation time of the carriers, when intense laser pulse irradiates more electron-hole pairs are generated and cause the states filling of CB and the bleaching of the VB. This will block the further absorption, resulting in the SA behavior [9, 23]. When rGO is decorated with Ag NPs, the metal states are flat and extend into that of rGO [24]. Owing to the considerably larger density of states in the metal, the excited electrons in the CB of rGO has higher probability of transferring to the metal than to the VB of rGO. Since the carriers are excited faster than their relaxation from the metal states to the VB of rGO, the bleaching of the ground state takes place, resulting in a stronger SA effect [9, 25]. It should be noted that, when the input pulse intensity is increased to several GW/cm^2, reversed saturable absorption (RSA) was observed, which could be attributed to two-photon absorption effect [26].

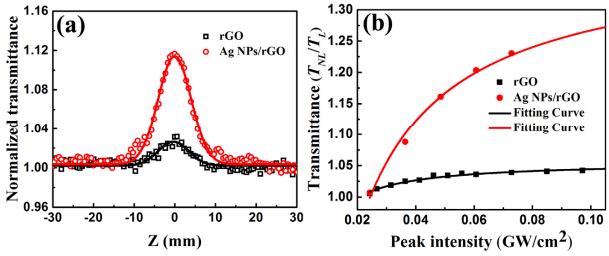

Fig. 3. (a) OA Z-scan measurement results of rGO and Ag NPs/rGO when the laser power was fixed at 72 MW/cm^2. (b) Normalized transmission as a function of input laser intensity for rGO and Ag NPs/rGO.

Closed aperture (CA) Z-scan measurements in rGO and Ag NPs/rGO are performed to verify the enhancement of nonlinear refraction effect of rGO functionalized with Ag NPs. In order to provide a reliable comparison, both rGO and Ag NPs/rGO are tested in the same experimental conditions. A typical peak-valley Z-scan trace resulting from the division of the

Optical Materials EXPRESS

CA Z-san data by the OA Z-san data for rGO and Ag NPs/rGO is depicted in Fig. 4. The measurement results are fitted theoretically using the formula from [16]:

$$T(x) = 1 + \frac{4x\Delta\Phi}{(1+x^2)(9+x^2)} \tag{4}$$

where $x = z/z_R$ is the normalized position to the Rayleigh length z_R and $\Delta\Phi = (2\pi/\lambda)n_2 L I_0$, with L and I_0 being the sample thickness and peak-on-axis intensity, which are estimated to be about of about 100 nm of 0.17 GW/cm^2, respectively. In our experiments, no obvious peak-valley was observed in the Z-scan trace of bare glass substrate, the response of glass substrate is negligible under the same experiment conditions. Both the divided Z-scan traces in rGO and Ag NPs/rGO recorded exhibit a pre-focal peak followed by a post-focal valley indicating the nonlinearity of the samples to be negative (negative nonlinear refraction). In our measurements, the peak-on-axis intensity was 0.17 GW/cm^2, the estimated value of the nonlinear refractive index n_2 of rGO is -4.9×10^{-13} m^2/W. The Ag NPs/rGO boosts the nonlinear refractive index as large as 2~3 times of that of rGO reaching to -1.1×10^{-12} m^2/W. It's believed that the nonlinear refraction of rGO is mainly attributed to the population redistribution of π electrons and the free carriers of the sp^2 domain [27]. As discussed above, when decorated with AgNPs and excited by the laser pulse, carriers are possible to transfer to the NPs metal states. The relative slow relaxation of the excited carriers from the metal states to the VB of rGO will cause the increase of the carrier density in the excited states [9, 23]. This might cause the enhancement of the nonlinear refractive index of the material.

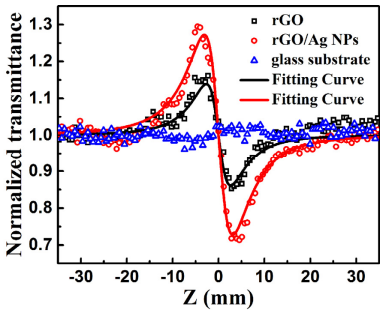

Fig. 4. Z-scan trace of rGO and Ag NPs/rGO resulting from the division of the CA data by the OA data. The theoretical fittings are indicated as solid lines.

4. Conclusions

In summary, we synthesized the reduced rGO decorated with Ag NPs by femtosecond laser ablation method. The nonlinear optical properties of both rGO and Ag NPs/rGO have been measured by Z-scan measurement. The results reveal both nonlinear absorption and nonlinear refraction can be effectively enhanced by the hybridization of Ag NPs. The results of power-dependent transmission indicate that the hybrid can provide saturable absorbers with higher modulation depth compared to that of rGO. The improvement of the SA of the hybrid is attributed to the charge transfer between Ag NPs and rGO. This also might cause the enhancement of the nonlinear refractive index of the material. The Ag NPs/rGO boosts the nonlinear refractive index as large as 2~3 times of that of the reference rGO reaching to -1.1×10^{-12} m^2/W at 800 nm femtosecond laser with 80 fs pulse duration.

Funding

National Natural Science Foundation of China (Grant No. 61427816, 11674260 and 11474078); Fundamental Research Funds for the Central Universities, and the collaborative Innovation Center of Suzhou Nano Science and Technology.